RESEARCH ARTICLE | OCTOBER 28 2024

Keeping dark modes dark: Reducing the effects of symmetry breaking at oblique incidence

Kieran J. Cowan ; Simon J. Berry ; Alastair P. Hibbins ; Alexander W. Powell

Appl. Phys. Lett. 125, 181101 (2024)
https://doi.org/10.1063/5.0227519

Applied Physics Letters ARTICLE pubs.aip.org/aip/apl

Keeping dark modes dark: Reducing the effects of symmetry breaking at oblique incidence

Cite as: Appl. Phys. Lett. **125**, 181101 (2024); doi: 10.1063/5.0227519
Submitted: 9 July 2024 · Accepted: 15 October 2024 ·
Published Online: 28 October 2024

Kieran J. Cowan,[1,a)] Simon J. Berry,[2] Alastair P. Hibbins,[1] and Alexander W. Powell[1]

AFFILIATIONS

[1]Department of Physics and Astronomy, Centre for Metamaterial Research and Innovation, University of Exeter, Stocker Road, Exeter EX4 4QL, United Kingdom
[2]QinetiQ, Farnborough, Hampshire GU14 0LX, United Kingdom

[a)]Author to whom correspondence should be addressed: kc485@exeter.ac.uk

ABSTRACT

Dark modes are defined by their lack of radiative coupling to the far field. However, the modes can be made to couple to far field radiation by symmetry breaking. For a resonant dimer, obliquely incident waves can create a phase difference in the currents between the elements, resulting in symmetry breaking. This work reduces symmetry breaking effects by minimizing the size of a dimer of dipolar elements with respect to its resonant wavelength. We obtain a mode that can experimentally be excited from the near field but has negligible excitation in the far field for obliquely incident waves. Such a mode could have use in wireless security applications.

Dark modes are resonances of a structure that by definition are non-radiative, meaning when illuminated by an incoming plane wave they do not radiatively couple to this field. Although in many cases, a small degree of symmetry breaking then enables the far field to excite the previously dark mode. The interaction of dark modes with the far field and their "bright" counterparts has held much interest in research over the years. For example, weak far field coupling of the mode due to symmetry breaking can provide the high Q-factors used in sensing[1–6] and the near field enhancement useful for second harmonic generation.[7] Another example is near field coupling between a bright mode and a dark mode can give an analog of electromagnetic induced transparency (EIT), which in turn can be used for sensing and slow light applications.[8–10]

In this study, we are interested in dimers of dipolar elements and their out-of-phase mode which is "dark"; the mode does not couple to the far field due to its zero net dipole moment.[11–13] As the two dipole elements couple to each other to form a dimer, the in-phase mode and the out-of-phase mode split in frequency.[14] The frequency splitting between these two modes depends on the coupling strength, which is primarily determined by the geometry and dipole separation.[2,11,13–15] The symmetry of a dimer system can be broken to gain a net dipole moment, which for example is used in obtaining high Q-factor modes and EIT-analog. A variety of methods have been developed to do so across a range of frequency regimes. An example of symmetry breaking by changing the dimer geometry is Panaro *et al.*[13] who rotate one of the dipoles with respect to the other, breaking rotational symmetry as the dipole moments are no longer in line. Other works, for example,[11,16] introduced a third resonator in different ways, all allowing excitation of the out-of-phase mode from the far field by breaking rotational symmetry. Excitation of the out-of-phase mode can also be obtained without geometric symmetry changes to the dimer, for example by having the incident radiation arrive at oblique incidence.[10,17] This forms a phase gradient across the structure, allowing for excitation of modes that otherwise have zero net dipole moment at normal incidence. In other words, in these structures the dark mode is only actually "dark" at normal incidence. Whereas previous work has focused on enabling weak coupling, our study wishes to reduce the coupling to dark modes via symmetry breaking that inherently exists due to oblique incidence, thus keeping the dark mode dark.

Anapoles are similar to dark modes but are a fundamentally different phenomena. Anapoles, despite far field coupling to the structure, do not scatter incident radiation.[3,18] Mikhailovskaya *et al.* suggest anapoles for use in wireless security applications,[19] where a device would operate using the anapole and so is intended to be accessible only from the near field. However, their design[19] required expensive ceramics and a spherical geometry, which could be considered impractical. A design that instead achieves no far field scattering using a resonator on a thin printed circuit board (PCB) material could therefore open up cheaper pathways for future research.

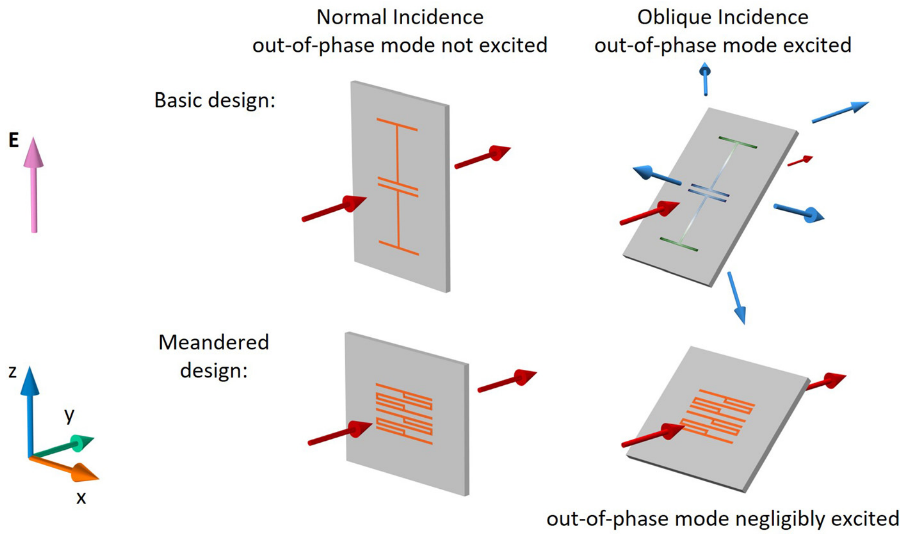

FIG. 1. Schematic illustrating normally and obliquely incident waves on the basic and meandered dimer designs. For a normally incident wave, the out-of-phase mode is not excited in either design. For an obliquely incident wave, the out-of-phase mode is now excited in the basic design but is negligibly excited in the meandered design.

In this paper, we designed a dimer of dipolar elements on a PCB with a mode that, regardless of the angle of the incident wave, is negligibly excited in the far field (as shown in Fig. 1). The simplest design for a dimer on PCB is a pair of thin rectangular metal wires. By extending the ends to form a "HH" shape (basic design in Fig. 1), we increased the coupling between the dipoles. For angles of incidence oblique to the design surface, the out-of-phase mode couples to free space due to the phase gradient; therefore, we modified the design to be more compact with respect to the resonant wavelength. This more-compact design reduces the phase gradient across the structure, weakening the excitation of the out-of-phase mode by an obliquely incident wave. The design was modified further by adding a meander (meandered design in Fig. 1) that again makes the dimer more compact. A schematic of the phase gradient across the basic and meandered designs can be found in the supplementary material. The compact and meandered designs were fabricated and probed in the near field and measured in the far field using a quasi-monostatic radar cross section (RCS) setup. In our results, as later shown, the out-of-phase mode in the meandered structure could be excited in the near field but is indistinguishable from background noise in the far field. This was regardless of the angle of incidence, and therefore we term the final design's out-of-phase mode an isotropic dark mode. This could be of use in future work in wireless security applications, where a device operates using an isotropic dark mode. Existing devices such as bank cards primarily operate in the low megahertz using spiral resonators that are magnetically induced and so are inherently near field.[20] Devices using electric fields are not used due to the possibility of unwanted access from the far field. Our device therefore presents an alternate pathway that would allow use of an electric field based device that carries reduced risk of unwanted far field access. That the out-of-phase mode near field coupling is dependent on the location of the probe with respect to the dimer also might be of use in such applications.

Samples used in experiments were etched, using a printed iron-on mask, from copper-clad Rogers RT/Duroid 5870 substrate (the PCB). Schematics in Figs. 2(a), 3(a), and 4(a) show the dimensions of

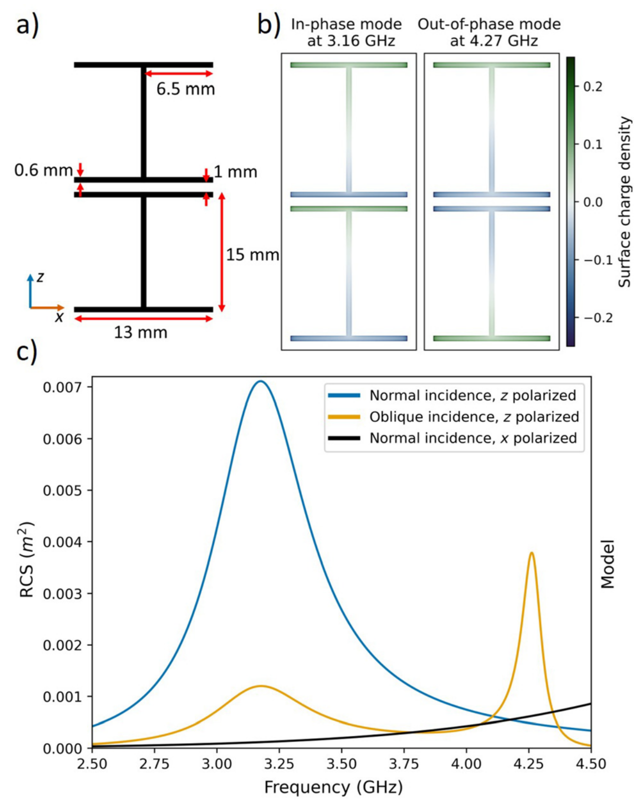

FIG. 2. (a) Schematic of the basic HH design with dimensions and axis orientation. (b) Surface charge density on the dimer for the in-phase and out-of-phase modes, obtained from an eigenfrequency model. Scale has been normalized to maximum magnitude value and saturated. (c) Plot of the modeled backscattered RCS vs frequency of a "HH"-shaped copper dimer on RT/Duroid 5870 substrate. This shows the response for z polarized waves normally and obliquely incident and x polarized waves normally incident.

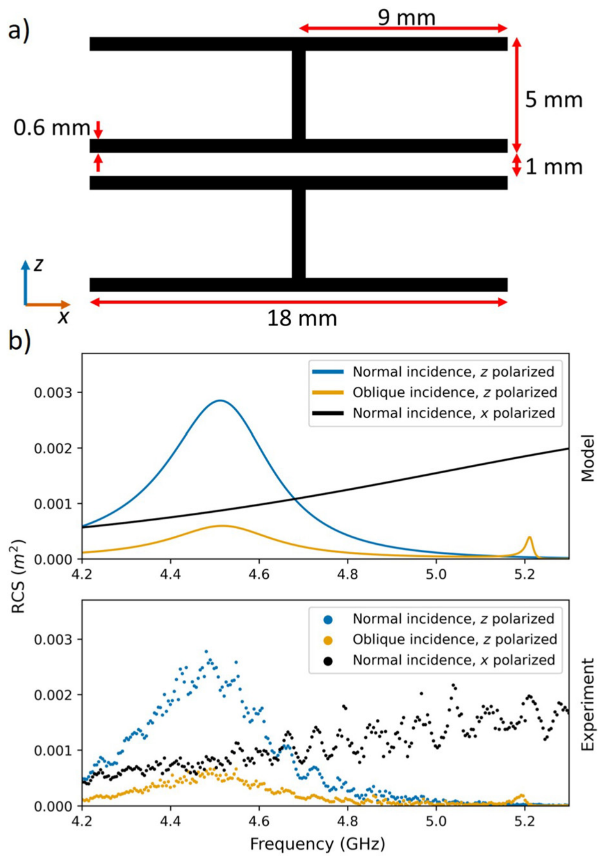

FIG. 3. (a) Schematic of the compact HH design with dimensions and axis orientation. (b) Plot of the modeled (top) and experimental (bottom) backscattered RCS vs frequency of a compact "HH"-shaped copper dimer on RT/Duroid 5870 substrate. This shows the response for z polarized waves normally and obliquely incident and x polarized waves normally incident.

the samples used in modeling with the designs labeled basic HH, compact HH, and meandered HH, respectively. Samples of the compact and meandered designs were fabricated; however, manufacturing limitations mean actual dimensions of the copper vary. For the fabricated meandered (compact) design, the width was on average 4 (15)% larger than the 0.6 mm modeled with a maximum that was 16 (30)% larger and a minimum that was 12 (0)% smaller. The modeled 18 mm lengths were on average those values, with a maximum that was 0.8 (0.7)% larger and a minimum that was 0.2 (0)% smaller. The substrate has a dielectric constant of $\epsilon_r = 2.33$. Its dissipation factor is linearly interpolated from $\tan\delta = 0.0005$ at 1 MHz to $\tan\delta = 0.0012$ at 10 GHz. Substrate thickness is 1.57 mm and copper thickness is 35 μm for all samples. Substrate dimensions are 30×45 mm for the basic HH design, 38×31 mm for the compact HH design, and the meandered HH design. A photo of the fabricated meandered design can be seen in Fig. 4(b).

Far field measurements were standard quasi-monostatic RCS that characterize the scattering of the resonator.[21] Flann Microwave dual polarized horns (Model DP240-AB) and an Anritsu ShockLine MS46122B 20 GHz Vector Network Analyzer (VNA) were used. The incident wave travels in the $+$y direction with the axis as depicted in schematics [Figs. 1, 2(a), 3(a), and 4(a)]. Measurements labeled z polarized are linearly polarized with E field aligned to the z axis, while those labeled x polarized have the E field aligned to the x axis. A schematic of the far field measurement experimental setup can be found in the supplementary material. The sample was rotated 45° about the x axis for measurement (and model) data labeled oblique, as this rotation would introduce a phase gradient that gives the out-of-phase mode a net dipole moment. While other rotations might introduce a phase gradient, 45° about the x axis was found to be the worst case as it gives the highest backscattered RCS magnitude, corresponding to the out-of-phase mode. In the supplementary material, we obtain a mathematical expression relating the net dipole moment to the angle of incidence. The expression supports that the out-of-phase mode's magnitude peaks at about 45° and that its net dipole moment will be smaller compared to the in-phase mode the more compact the structure is with respect to the resonant wavelength.

Near field measurements were performed by placing a probe at different locations around the sample, labeled i, ii, and iii, as marked in Fig. 4(a). A rigid copper sheathed coaxial cable was stripped back to leave its center, a stub of copper galvanized in aluminum, 3.1 mm in length, forming the probe. The remaining copper sheathed coaxial was sandwiched between sheets of microwave absorbing foam (ABS technics, ABS-ASF-12 foam) to attenuate waves that formed along its outer surface. The tip of the probe was placed approximately 1 mm away from the sample and perpendicular to its surface. The measured S_{11} was normalized to the probe in free space. An Antritsu MS4644A 40 GHz VNA was used.

Experimental results are compared to finite element method numerical models.[22] Surface charge densities obtained from eigenfrequency models have been normalized to their maximum magnitude values and then the color scale saturated to aid visual representation in Figs. 1, 2(b), and 5(a). The conductivity of copper was modeled as 5.998×10^7 S/m.

The design shown in Fig. 2(a) is our basic HH dimer that acts as our starting point. An eigenfrequency model of the structure gives the in-phase mode at 3.16 GHz and the out-of-phase mode at 4.27 GHz with surface charge densities shown in Fig. 2(b). The modeled RCS of the basic HH dimer for z polarization at normal incidence in Fig. 2(c) shows a peak corresponding to the in-phase mode at 3.18 GHz, however, a peak is not seen at 4.27 GHz because the out-of-phase mode has zero net dipole moment. When the sample is rotated 45° about the x axis, a peak corresponding to the out-of-phase mode appears at 4.26 GHz, with a magnitude that is approximately 53% of that of the in-phase mode. Due to weaker coupling to the far field, the out-of-phase mode has a higher Q-factor than the in-phase mode. In sensing applications, these high Q-factors are obtained at normal incidence through symmetry breaking.[5,6,13] As this work is focused on suppressing symmetry breaking, we use a symmetric structure to prevent coupling to the out-of-phase mode at normal incidence. However, when the sample is rotated, a phase gradient is introduced in the incident electric field across the sample that in turn creates a phase difference in the currents. This phase gradient has given the out-of-phase mode of our initial design a net dipole moment and so it is no longer dark. We want to reduce this excitation due to the angle of the incident wave. To this end, we want to reduce the phase difference in the currents for the two dipoles under rotation.

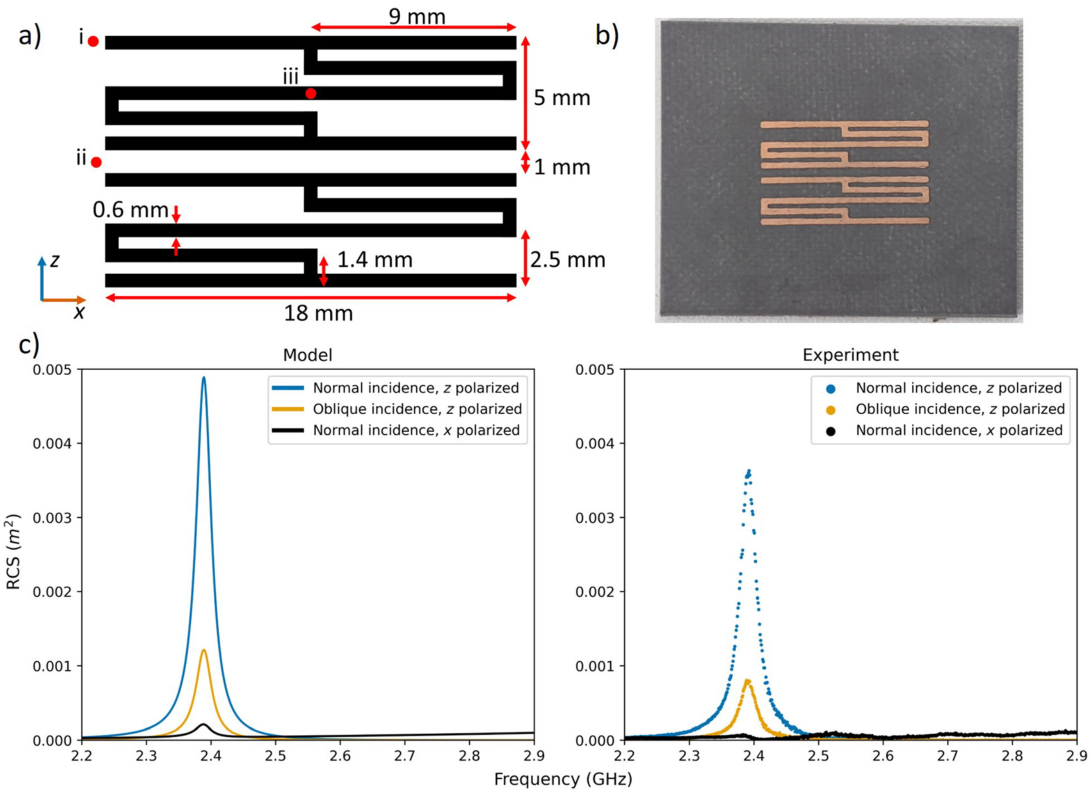

FIG. 4. (a) Schematic of the meandered HH design with dimensions and axis orientation. The points labeled i, ii, and iii show locations for the near field probe. (b) Photo of the fabricated sample for the meandered HH design. (c) Plots of the modeled (left) and experimental (right) backscattered RCS vs frequency of our meandered "HH"-shaped copper dimer on RT/Duroid 5870 substrate. This shows the response for z polarized waves normally and obliquely incident and x polarized waves normally incident.

In order to reduce the phase difference, we make the resonator more geometrically compact with respect to the resonant wavelength. Still keeping a "HH" shape, the length is increased in the end plates but reduced along the dimer axis to the dimensions given in Fig. 3(a). Due to changes in overall length, self inductive (L) and capacitive (C) effects, the resonant frequencies are shifted compared to the basic HH design. The changes to L and C influence the resonant frequency by $f = 1/\sqrt{LC}$ according to circuit theory that is often used to represent microwave resonators.[21] The RCS of this compact design, obtained from both experiment and modeling, is shown in Fig. 3(b). The experimental data show peaks that are shifted 0.02 GHz lower compared to the model. This is on the scale of shift expected from fabrication tolerances and substrate permittivity error. The magnitude of the RCS is lower in experiment than in model data, an effect that was attributed to the surface roughness of the copper giving a lower effective conductivity than that which was modeled.[23] The oscillations in the data are attributed to a standing wave forming in the anechoic chamber. For the model, once again with z polarization and normal incidence there is a peak corresponding to the in-phase mode at 4.51 GHz and no sign of the out-of-phase mode. Upon rotating the structure 45° about the x axis the peak corresponding to the out-of-phase mode appears at 5.21 GHz, this time with an RCS that is approximately 14% of that of the peak of the in-phase mode, showing the symmetry breaking effect has been reduced. Considering an x polarized incident wave, at 5.21 GHz the RCS has a magnitude that is approximately 66% of the peak corresponding to the in-phase mode. The mode excited by a x polarized incident wave has the current travel only along the 18 mm lengths of the HH shape, whereas for z polarization the current is in both the 5 and 18 mm lengths. Therefore, geometry changes have made the lengths the current travels similar for both x and z polarizations, so the different modes excited by each polarization are now closer in resonance than in the basic HH design. Therefore, to obtain negligible far field coupling at the out-of-phase mode frequency, we want to make the structure more geometrically compact with respect to resonant wavelength and negate the modes excited by a x polarized incident wave.

Our solution was to add a meander to the central track of the design, as shown with dimensions in Fig. 4(a). For a x polarized incident wave, the current is still along the 18 mm lengths, so the meander does not shift the resonant frequency of the modes. For a z polarized incident wave, the current will travel the additional length of the meander, shifting the modes to lower frequencies. In this meandered design we have duplicated and translated the dipole down in z coordinate to create its paired element. We also modeled a meandered design where the dipoles were instead mirrored in the x axis. While mirror symmetry is kept in this other design, rotational symmetry is broken and so for a normally incident x polarized wave, the out-of-phase mode is excited with non-negligible RCS magnitude. For this reason,

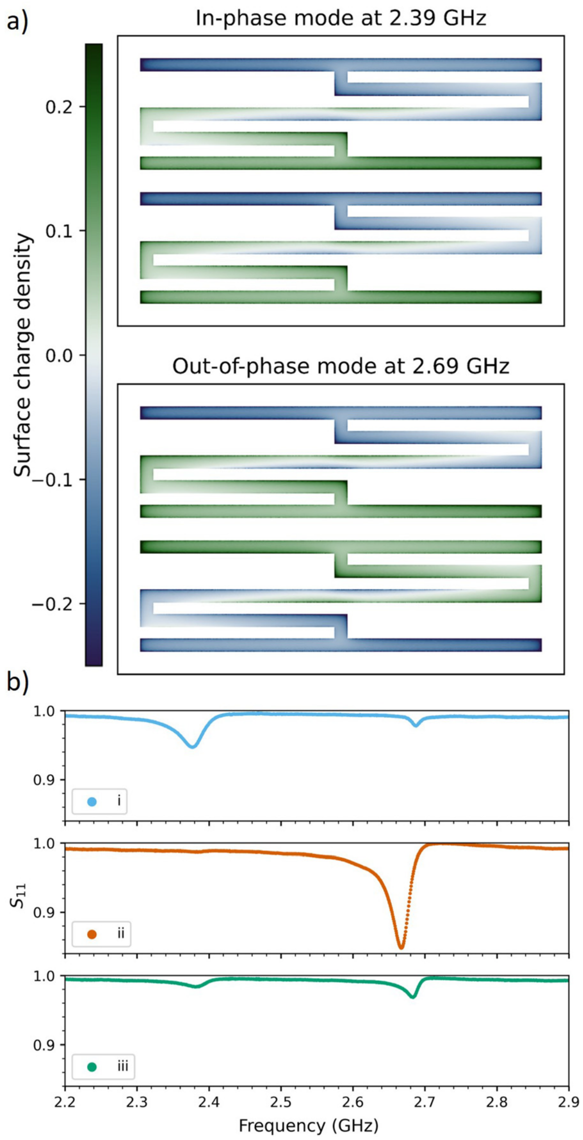

FIG. 5. (a) Surface charge density on the dimer for the in-phase and out-of-phase modes, obtained from an eigenfrequency model. Scale has been normalized to maximum magnitude value and saturated. (b) Plot of the measured S_{11} from our near field experiment of our meandered "HH"-shaped copper dimer on RT/Duroid 5870 substrate. Labels i, ii, and iii refer to different locations on the sample [see Fig. 4(a)].

we have chosen the translated version of the meandered dimer, to maximize dark mode suppression. The length of the meander was chosen so that it shifts the modes while still fitting in the same dimensions as the compact design.

By shifting the resonances down in frequency and leaving the dimer length (11 mm) unchanged, we have made the structure more compact with respect to the resonant wavelength. Figure 4(c) shows the experimental and modeled RCS of the meandered design. The experimental data are shifted 0.004 GHz lower than the model, which again is on the scale of shift expected from fabrication tolerances and substrate permittivity error. We provide further information on the effect of tolerances on a group of duplicate samples in the supplementary material. Again, the RCS magnitude being lower in experiments was attributed to the effects of surface roughness on conductivity.[23] The model RCS shows a peak corresponding to the in-phase mode at 2.39 GHz. An eigenfrequency model gives the out-of-phase mode to be at 2.69 GHz, yet there is no corresponding peak in RCS to that seen in the previous designs for oblique incidence. For a x polarized incident wave, the magnitude at the frequency of the out-of-phase mode has decreased to approximately 1% of the peak corresponding to the in-phase mode. With negligible RCS magnitude at the out-of-phase mode, we have reduced symmetry breaking effects that usually arise from an obliquely incident wave, resulting in an isotropic dark mode.

To support the idea of the isotropic dark mode being used in wireless security applications, we want to show there is still near field excitation of the out-of-phase mode. A near field device could then operate using the out-of-phase mode. Eigenfrequency models of the meandered design give the in-phase mode at 2.39 GHz and the out-of-phase mode at 2.69 GHz, with surface charge densities shown in Fig. 5(a). Figure 5(b) shows the S_{11} measured in the near field at the locations marked in Fig. 4(a). We measure a dip corresponding to the in-phase mode at 2.38 GHz and another that corresponds to the out-of-phase mode at 2.69 GHz. Whether a mode is excited or not depends on the location of the probe, as was expected based on the work of Gao *et al.*[11] When the probe is at location ii, the closest two end plates have the opposite sign charge, making the out-of-phase mode strongly excited. The probe being at locations i or iii supports either charge configuration.

In literature, dark modes can be made bright through breaking the symmetry conditions, such as the angle of incidence, that give them their zero net dipole moment. This work has instead explored reducing the effects of symmetry breaking that occurs from obliquely incident waves on a dark mode supporting structure, resulting in an isotropic dark mode that is negligibly excited in the far field from any angle of incident wave. A design of a resonant "HH"-shaped dimer whose out-of-phase mode is a dark mode that is angle dependent was used as a starting point. Keeping the overall "HH" shape, the design was made more geometrically compact with respect to the resonant wavelength. This reduced the symmetry breaking effects observed in RCS due to oblique incidence but led to an increase in the RCS at the frequency of the out-of-phase mode due to modes excited by the orthogonal polarization. So, the design was modified further by adding a meander to the central length of the "H"-shaped dipoles, shifting modes apart and increasing how compact the dimer is with respect to the resonant wavelength. We fabricated this meandered design and experimentally measured it in the near and far fields. Experiments and models showed near field excitation but negligible far field RCS regardless of incident wave angle or orientation at the frequency of the out-of-phase mode. Future work could explore the integration of such a structure into wireless security applications, where it might allow for near field only operation by using the dark mode that has negligible excitation for obliquely incident waves.

See the supplementary material for additional information on the far field experimental setup, phase gradient, fabrication tolerances, and a mathematical relationship between angle of incidence and net dipole moment.

This work is supported by an ICASE from the Engineering and Physical Sciences Research Council (EPSRC) and QinetiQ (Grant No. EP/X524906/1, Voucher No. 220181).

AUTHOR DECLARATIONS

Conflict of Interest

The authors have no conflicts to disclose.

Author Contributions

Kieran J. Cowan: Conceptualization (equal); Data curation (lead); Formal analysis (lead); Investigation (lead); Methodology (lead); Validation (lead); Visualization (lead); Writing – original draft (lead). **Simon J. Berry:** Conceptualization (supporting); Project administration (supporting); Resources (supporting); Supervision (supporting); Writing – review & editing (equal). **Alastair P. Hibbins:** Conceptualization (equal); Funding acquisition (equal); Project administration (equal); Resources (equal); Supervision (equal); Writing – review & editing (equal). **Alex W. Powell:** Conceptualization (equal); Funding acquisition (equal); Project administration (equal); Resources (equal); Supervision (equal); Writing – review & editing (equal).

DATA AVAILABILITY

The data that support the findings of this study are available from the corresponding author upon reasonable request.

REFERENCES

[1]S. Banerjee, C. Amith, D. Kumar *et al.*, "Ultra-thin subwavelength film sensing through the excitation of dark modes in THz metasurfaces," Opt. Commun. **453**, 124366 (2019).

[2]K. Q. Le, A. Alù, and J. Bai, "Multiple Fano interferences in a plasmonic metamolecule consisting of asymmetric metallic nanodimers," J. Appl. Phys. **117**, 023118 (2015).

[3]F. Monticone, D. Sounas, A. Krasnok *et al.*, "Can a nonradiating mode be externally excited? nonscattering states versus embedded eigenstates," ACS Photonics **6**, 3108–3114 (2019).

[4]K. Koshelev, G. Favraud, A. Bogdanov *et al.*, "Nonradiating photonics with resonant dielectric nanostructures," Nanophotonics **8**, 725–745 (2019).

[5]Y. Gao, J. Ge, S. Sun *et al.*, "Dark modes governed by translational-symmetry-protected bound states in the continuum in symmetric dimer lattices," Results Phys. **43**, 106078 (2022).

[6]K. Koshelev, S. Lepeshov, M. Liu *et al.*, "Asymmetric metasurfaces with high-Q resonances governed by bound states in the continuum," Phys. Rev. Lett. **121**, 193903 (2018).

[7]K. Thyagarajan, J. Butet, and O. J. F. Martin, "Augmenting second harmonic generation using Fano resonances in plasmonic systems," Nano Lett. **13**, 1847–1851 (2013).

[8]K. Jin, X. Yan, X. Wang *et al.*, "Dark mode tailored electromagnetically induced transparency in terahertz metamaterials," Appl. Phys. B **125**, 68 (2019).

[9]Z. He, H. Li, S. Zhan *et al.*, "Combined theoretical analysis for plasmon-induced transparency in waveguide systems," Opt. Lett. **39**, 5543 (2014).

[10]W. Khunsin, J. Dorfmüller, M. Esslinger *et al.*, "Quantitative and direct near-field analysis of plasmonic-induced transparency and the observation of a plasmonic breathing mode," ACS Nano **10**, 2214–2224 (2016).

[11]Y. Gao, N. Zhou, Z. Shi *et al.*, "Dark dimer mode excitation and strong coupling with a nanorod dipole," Photonics Res. **6**, 887 (2018).

[12]S. Lee, Y. Park, J. Kim *et al.*, "Selective bright and dark mode excitation in coupled nanoantennas," Opt. Express **26**, 21537 (2018).

[13]S. Panaro, A. Nazir, C. Liberale *et al.*, "Dark to bright mode conversion on dipolar nanoantennas: A symmetry-breaking approach," ACS Photonics **1**, 310–314 (2014).

[14]P. Nordlander, C. Oubre, E. Prodan *et al.*, "Plasmon hybridization in nanoparticle dimers," Nano Lett. **4**, 899–903 (2004).

[15]M. Parise and G. Antonini, "On the inductive coupling between two parallel thin-wire circular loop antennas," IEEE Trans. Electromagn. Compat. **60**, 1865–1872 (2018).

[16]D. E. Gómez, Z. Q. Teo, M. Altissimo *et al.*, "The dark side of plasmonics," Nano Lett. **13**, 3722–3728 (2013).

[17]E. Bochkova, S. N. Burokur, A. de Lustrac *et al.*, "Dark mode engineering in metasurfaces by symmetry matching approach," Appl. Phys. A **124**, 119 (2018).

[18]Y. Yang and S. I. Bozhevolnyi, "Nonradiating anapole states in nanophotonics: From fundamentals to applications," Nanotechnology **30**, 204001 (2019).

[19]A. Mikhailovskaya, D. Shakirova, S. Krasikov *et al.*, "Anapole-enabled RFID security against far-field attacks," Nanophotonics **10**, 4409–4418 (2021).

[20]D. Dobkin, *The RF in RFID: UHF RFID in Practice* (Elsevier Science, 2012), pp. 24–34.

[21]D. M. Pozar, *Microwave Engineering* (John Wiley & Sons, Inc., 2012), pp. 272–275.

[22]COMSOL AB, *COMSOL Multiphysics® v. 6.2* (COMSOL AB, Stockholm, Sweden, 2023). www.comsol.com

[23]B. Huang and Q. Jia, "Accurate modeling of conductor rough surfaces in waveguide devices," Electronics **8**, 269 (2019).